IRIS AperTO

UNIVERSITÀ DEGLI STUDI DI TORINO

AperTO - Archivio Istituzionale Open Access dell'Università di Torino

The pitfalls of in vivo imaging techniques: evidence for cellular damage caused by synchrotron X-ray computed micro-tomography.

This is the author's manuscript

Original Citation:

Availability:

This version is available http://hdl.handle.net/2318/1734690 since 2021-11-15T14:56:45Z

Published version:

DOI:10.1111/nph.15368

Terms of use:

Open Access

Anyone can freely access the full text of works made available as "Open Access". Works made available under a Creative Commons license can be used according to the terms and conditions of said license. Use of all other works requires consent of the right holder (author or publisher) if not exempted from copyright protection by the applicable law.

(Article begins on next page)

04 February 2023

The pitfalls of *in vivo* imaging techniques: evidence for cellular damage caused by synchrotron X-ray computed micro-tomography

F. Petruzzellis[1], C. Pagliarani[2,5], T. Savi[1,3], A. Losso[4], S. Cavalletto[5], G. Tromba[6], C. Dullin[6,7,8], A. Bär[4], A. Ganthaler[4], A. Miotto[1], S. Mayr[4], M.A. Zwieniecki[9], A. Nardini[1]*, F. Secchi[5]

1. Dipartimento di Scienze della Vita, Università di Trieste, Via L. Giorgieri 10, 34127 Trieste, Italia
2. Institute for Sustainable Plant Protection, National Research Council, Strada delle Cacce 73, 10135 Torino, Italia
3. University of Natural Resources and Life Sciences, Division of Viticulture and Pomology, Department of Crop Sciences, Konrad Lorenz Straße 24, A-3430 Tulln, Vienna, Austria
4. Department of Botany, University of Innsbruck, Sternwartestraße 15, 6020 Innsbruck, Austria
5. Dipartimento di Scienze Agrarie, Forestali e Alimentari, Università di Torino, Largo Paolo Braccini 2, 10095 Grugliasco (TO), Italia
6. Elettra-Sincrotrone Trieste, Area Science Park, 34149 Basovizza, Trieste, Italia
7. Institute for Diagnostic and Interventional Radiology, University Medical Center Göttingen, Robert-Koch-Straße 40, 37075 Göttingen, Germany
8. Max-Plank-Institute for Experimental Medicine, Hermann-Rein-Straße 3, 37075 Göttingen, Germany
9. Department of Plant Sciences, University of California Davis, One Shields Ave, Davis, CA 95616, USA

* Corresponding author: nardini@units.it

ABSTRACT

- Synchrotron X-ray computed micro-tomography (microCT) has emerged as a promising non-invasive technique for *in vivo* monitoring of xylem function, including embolism build-up under drought and hydraulic recovery following re-irrigation. Yet, the possible harmful effects of ionizing radiation on plant tissues have never been quantified.

- We specifically investigated the eventual damage suffered by stem living cells of three different species exposed to repeated microCT scans. Stem samples exposed to one, two or three scans were used to measure cell membrane and RNA integrity, and compared to controls never exposed to X-rays.

- Samples exposed to microCT scans suffered serious alterations to cell membranes, as revealed by marked increase in relative electrolyte leakage, and also underwent severe damage to RNA integrity. The negative effects of X-rays were apparent in all species tested, but the magnitude of damage and the minimum number of scans inducing negative effects were species-specific.

- Our data show that multiple microCT scans lead to disruption of fundamental cellular functions and processes. Hence, microCT investigation of phenomena that depend on physiological activity of living cells may produce erroneous results and lead to incorrect conclusions.

INTRODUCTION

In plants, long distance water transport relies on transmission of transpiration-induced negative pressure (= tension) via the xylem conduits connecting root tips to leaf cells (Jensen *et al.*, 2016). Such a fascinating mechanism has the important drawback to be metastable and vulnerable to liquid-to-vapor transition, leading to the blockage of water transport (Zimmermann, 1983). Most frequently, this happens when air is aspirated through inter-conduit pit membranes into water-filled conduits experiencing critical tensions (Shen *et al.*, 2015; Zwieniecki & Secchi, 2015). Increased frequency of drought and heat waves is accelerating plant mortality rates worldwide (Hember *et al.*, 2017), and hydraulic failure has emerged as the main cause (Anderegg *et al.*, 2011). A detailed knowledge of species-specific vulnerability to xylem embolism (Maherali *et al.*, 2004), and of the eventual capacity for hydraulic recovery (Mayr *et al.*, 2014; Secchi *et al.*, 2017; Klein *et al.*, 2018) is crucial to improve projections of forest and crop resistance/resilience under future climate scenarios.

Techniques used to measure plant hydraulic conductance upon drought and recovery are generally destructive (Cochard *et al.*, 2013). Stems, roots, petioles and even leaves are excised from plants during or after drought stress, and connected to hydraulic systems to measure flow rates across samples under known pressure differences (Sperry *et al.*, 1988). Alternatively, tissues can be infiltrated with dyes to distinguish functioning *versus* embolized or otherwise non-conducting conduits (Ewers & Fisher, 1989). Due to negative pressure in functional xylem conduits, samples' excision might cause air entry in the xylem, producing artefactual embolism (Wheeler *et al.*, 2013). The magnitude of this artefact may depend on xylem pressure at sampling time and on conduit length (Beikircher & Mayr, 2016). Although several studies found no striking evidence for artefacts associated with classical hydraulic techniques (Jacobsen & Pratt, 2012; Trifilò *et al.*, 2014; Fukuda *et al.*, 2015; Hacke *et al.*, 2015; Scoffoni & Sack, 2015; Venturas *et al.*, 2015; Ogasa *et al.*, 2016; Nardini *et al.*, 2017; Nolf *et al.*, 2017), it is conceivable that estimates of xylem vulnerability to embolism and restoration of xylem functionality (recovery) (Nardini *et al.*, 2018), are biased by destructive sampling protocols.

These controversies have contributed to move forward the field of plant hydraulics (Jansen *et al.*, 2015; Venturas *et al.*, 2017), and stimulated the use of non-destructive techniques for *in vivo* monitoring of xylem function, like magnetic resonance imaging (Zwieniecki *et al.*, 2013), X-ray computed micro-tomography (microCT; Brodersen *et al.*, 2010), and the optical method applied to leaf venation (Brodribb *et al.*, 2016). In particular, microCT has emerged as a very promising technology, due to relatively ease of use, high spatial and temporal resolution, good contrast between air-filled and water-filled spaces, and fast scan times (Dhondt *et al.*, 2010; Pajor *et al.*, 2013; Cochard et al., 2015). Due to its supposed non-invasive nature, microCT has been suggested to

represent a reference technique to determine xylem vulnerability to embolism (Cochard *et al.*, 2015), and the eventual refilling of embolized conduits which supposedly relies on the activity of living xylem parenchyma cells (Tyree *et al.*, 1999; Brodersen & McElrone, 2013; Secchi *et al.*, 2017; Nardini *et al.*, 2018). While some studies demonstrated the occurrence of conduit refilling (Brodersen *et al.*, 2010; Brodersen *et al.*, 2018), others failed to detect hydraulic recovery following drought and re-irrigation (Choat *et al.*, 2015; Knipfer *et al.*, 2015; Charrier *et al.*, 2016; Hochberg *et al.*, 2016).

These contrasting findings raise questions about possible factors affecting the reliability of microCT observations (Pratt & Jacobsen, 2018). An obvious but often overlooked drawback of microCT is the use of X-ray sources and the potential tissue damage caused by the ionizing radiation (Han & Yu, 2009; Daly, 2012). Although this has been considered a minor issue because of short scan times, some studies on animal organisms indicated irreversible cellular damage even by exposure to very low X-ray doses (Rothkamm & Löbrich, 2003; Nguyen *et al.*, 2015). However, respective X-rays effect on plant samples have never been investigated in details, although previous studies indicated damage of plant tissues after microCT scans. As an example, Charrier *et al.* (2016) used vital staining to assess the functional status of stem parenchyma cells after exposure to X-rays, showing that several cells were damaged. Similarly, Savi *et al.* (2017) reported shrinkage and brownish scar formation in sunflower stems exposed to X-rays. Hence, it is very important and urgent to test eventual negative or otherwise undesired effects of X-rays on the observed samples, considering the raising importance of microCT as a tool for studies on plant hydraulic functioning. Here, we discuss the results from an experiment specifically designed to assess eventual damage to stem living cells during repeated microCT scans.

MATERIALS AND METHODS

Plant material

Experiments were performed on three species: *Helianthus annuus*, *Coffea arabica* cv. Pacamara, and *Populus tremula x alba*. *H. annuus* plants were six-week old, with a height of about 20 cm and a stem diameter of 2-3 mm at root collar. *C. arabica* plants were part of a collection of coffee cultivars hosted by Univ. Trieste. Experimental plants were three-year-old, with a height of 20-30 cm, and a stem diameter of 3-4 mm. Plants of *P. tremula x alba* were three-months-old, approximately 50 cm tall with a stem diameter of 3-4 mm.

All plants were maintained in a greenhouse at Univ. Trieste for 4 weeks before experiments (end of September 2017), and regularly watered. Air temperature and relative humidity averaged 16.5 °C and 60%, respectively. Mean daily photosynthetic photon flux density (PPFD) was 150 µmol m^{-2} s^{-1} (maximum 400 µmol m^{-2} s^{-1}).

115

116 Experimental setup

117 Experiments were performed at the SYRMEP beamline, Elettra Sincrotrone Trieste
118 (www.elettra.trieste.it). Two silicon filters (0.5 mm each) were used to obtain an average X-ray
119 source energy of 25 keV, resulting in an entrance dose rate in water of 47 mGy s^{-1}. X-ray window was
120 4 mm in height with horizontal opening up to 120 mm. Initial experiments were performed on intact
121 plants of *H. annuus* and *P. tremula x alba* (n = 3) to test for eventual over-heating of stems as a
122 possible factor inducing damage during scans. A type T thermocouple connected to a datalogger
123 (1000 Series Squirrel, Eltek) was inserted in the stem at half height. The plant was placed on the
124 sample holder and the stem was aligned with the beam. The beam was turned off to allow
125 temperature equilibration for 5 min. Then, the stem was irradiated for 10 min at a position located 8
126 mm above the thermocouple insertion point, while temperature was continuously recorded. After a
127 5 min interval without beam, the stage was moved upward and the stem was irradiated 3 mm above
128 the thermocouple, for another 10 min. The procedure was repeated by directly irradiating the
129 thermocouple insertion point.

130 The cellular damage caused by microCT scans was assessed by measuring cell membrane
131 integrity estimated by relative electrolyte leakage (REL), and level of RNA degradation on irradiated
132 stem tissues. Stem segments with a length of 1 cm (n = 5) were obtained from the mid portion of
133 stems of well hydrated plants, and immediately wrapped in Parafilm® in groups of 5 (sampled from 5
134 different plants). This allowed to prevent desiccation during storage (see below) and to irradiate
135 more samples during each scan. For each species, 14 sample sets (each with 5 stem pieces) were
136 prepared (total of 70 stem samples per species).

137 Samples were subjected to microCT scans while horizontally oriented to assure that all cells
138 were exposed to X-rays during the 360° rotation (the position was checked via real-time
139 visualization). The exposure time was set at 100 ms, at an angular step of 2° s^{-1} resulting in 3 min
140 scan. Samples were then used to measure REL (7 sets) and RNA quality (7 sets), according to
141 experimental design presented in Fig. 1. Exposed samples were tested after one, two, or three
142 consecutive scans at 90 minutes intervals (E1, E2, and E3). Controls (C0, C1, C2, C3) were never
143 exposed to irradiation. Time of exposure and beam energy level was similar to previously reported
144 experiments (e.g. Charrier *et al.*, 2016), although not all experiments are provided with energy level
145 parameter.

146 The integrity of cell membranes was estimated via REL measurements. C or E samples were
147 placed in 1.5 ml vials (1 segment per vial) with 1 ml of deionized water. In the case of *C. arabica* and
148 *P. tremula x alba*, segments were split longitudinally immediately before immersion to favor contact
149 between stem cells and the solution, as preliminary experiments showed that the bark delayed

150 solute diffusion. The tubes were shaken for 30 min at laboratory temperature. The initial electrical
151 conductivity (C_i) of the solution was measured (Twin Cond B-173, Horiba, Kyoto, Japan) using a 10 µl
152 aliquot. Samples were then subjected to 3 freezing-thawing cycles (1 min in liquid nitrogen followed
153 by 30 min at laboratory temperature), shaken for 5 min, and the final electrical conductivity was
154 measured (C_f) on another 10 µl aliquot. REL was finally calculated as (C_i/C_f) × 100 (Savi *et al.*, 2016).
155 For RNA analysis, frozen stems for each species and treatment were pooled and ground in
156 sterile mortars using liquid nitrogen followed by tissue lysing (TissueLyser II, Qiagen). Total RNA was
157 extracted following Chang *et al.* (1993), and RNA quantity and quality were determined
158 spectrophotometrically by NanoDrop (Thermo Fisher Scientific). RNA integrity (expressed as RNA
159 integrity number, RIN; Schroeder *et al.*, 2006) was finally inspected using the RNA 6000 Nano kit and
160 the Agilent 2100 Bioanalyzer (Agilent Technologies), according to manufacturer's instructions. The
161 RNA Integrity Number (RIN) is a standard reference for RNA quality assessment, specifically
162 introduced in routine RNA quality control processes to avoid subjective interpretation of results. The
163 RIN values resulting at the end of each Bionalyzer run provide a classification of total RNA quality,
164 based on a numbering system ranging from 1 (poor quality and high level of degradation) to 10 (high
165 quality and high integrity levels). As RNA degradation proceeds, there is a decrease in the 18S to 28S
166 ribosomal RNA band ratio and an increase in the background noise between the 18 and 28 ribosomal
167 peaks (Bioanalyzer user guide). In Fig. 4, the 18S ribosomal band is visible at 40-42 s time, while the
168 28S ribosomal band at 46 s time.
169
170 Statistical analysis
171 One-way parametric ANOVA analysis was run separately for each species to test differences between
172 REL values measured in C and E samples through "aov" function in "stats" package for R software (R
173 Development Core Team 2017). Data were log transformed to meet assumptions of normality and
174 homoscedasticity of variance. Post-hoc Tukey's Honestly Significant Differences comparisons were
175 run through "TukeyHSD" function in "stats" package for R.
176
177 **RESULTS**
178
179 Exposing stems of *H. annuus* or *P. tremula x alba* to X-rays did not did not result in biologically
180 significant changes in tissue temperature (Fig. 2). Stem temperature oscillated between 25 and 26 °C
181 with no beam, and no change was detected at a distance of 3 or 8 mm from the irradiated point even
182 under prolonged exposure (10 min). Temperature in stem section directly exposed to radiation rose
183 by about 1°C in both tested species.

Cell membrane integrity, quantified via REL measurements, was affected by X-ray exposure in analyzed species (Fig. 3). In all plants, REL of C0 samples was about 25%, and this value did not change significantly as a function of time from excision in C1, C2 and C3 samples (Fig. 3). In the case of *H. annuus*, the first scan did not induce changes in REL, however these became apparent in E2 and E3, when REL peaked to 70%, with some samples reaching values as high as 90%. In *P. tremula x alba*, REL increased to 35% in E2, and remained similar in E3. In *C. arabica* an increase of REL to 45% (albeit not significant due to large data variability) was already observed in E1 samples, reaching values > 50% in E3.

Total RNA quality was estimated by the RNA Integrity Number (RIN), as this is a reliable proxy to compare the integrity of RNA in different samples. Analyses based on this metric confirmed the results obtained by REL measurements, showing similar variability and resistance of species to radiation (Fig. 4). In the case of *H. annuus*, the first scan did not affect RNA quality (E1, 7.5). However, RNA degradation increased after the second exposure, and the RNA after the third exposure (E3) was almost fully degraded (Fig. 4). In this species, the controls (C0-C3) showed no degradation of RNA quality. There was no effect of time or X-ray exposures on RNA quality of samples collected from P*. tremula x alba* stems, although E3 samples had slightly lower RNA quality (RIN 6.2; Fig. 4). After one scan, RNA extracted from *C. arabica* was partially degraded (E1; RIN 4.1), in comparison to controls (C1, RIN 7). However, both X-ray exposures and time from excision influenced the RNA quality in this species (see C2-3 and E2-3; Fig. 4) confirming that *C. arabica* was sensitive to both manipulation and X-rays.

DISCUSSION

X-ray microCT is emerging as an important new tool for the visualization and quantification of xylem embolism (Cochard *et al.*, 2015). Based on its supposed non-invasive nature, microCT has also been used to visualize eventual post-drought embolism recovery. In both cases, plants are generally exposed to successive microCT scans to check embolism build-up during plant dehydration (Choat *et al.*, 2016), or its reversal following re-watering (Charrier *et al.*, 2016).

Xylem conduits are frequently considered as inert pipelines, but long-distance water transport relies on the activity of phloem and parenchyma, e.g. for the regulation of xylem sap ionic content (Zwieniecki *et al.*, 2001; Nardini *et al.*, 2011), modulation of xylem sap surface tension (Losso *et al.*, 2017), release of sugars and water during the refilling of embolized conduits (Secchi *et al.*, 2017), and production of conduit-filling exudates as a response to wounds (Jacobsen *et al.*, 2018). Hence, any eventual damage to living cells can be suspected to alter xylem function, thus casting doubts on the reliability of techniques inducing harmful effects on phloem or parenchyma. Our data

clearly show that microCT scans produce severe cellular damage, and call for renewed caution in the interpretation of findings based on this technique (Pratt & Jacobsen, 2018). The X-ray energy level and scan times in our experiment were similar to or even lower than those used in several recent studies (e.g. Charrier *et al.*, 2016; Choat *et al.*, 2016; Knipfer *et al.*, 2017). Yet, the X-ray dose was high enough to induce damage to both cell membranes and RNA.

Samples exposed to microCT scans showed significant increases in REL, indicating serious alterations to cell membranes. This is not surprising, as several studies have shown that X-rays produce irreversible damage to membrane lipid bilayers due to phase transformation and lamellar stacking (Köteles, 1982; Cheng & Caffrey, 1996; Cherezov *et al.*, 2002), with consequent effects on membrane permeability (Cao *et al.*, 2015). Cherezov *et al.* (2002) reported that membrane damage is not associated to temperature effects during sample irradiation at synchrotron light sources, as also confirmed by the lack of over-heating recorded in our samples, but it rather depends on generation of free radicals. Most importantly, Cherezov *et al.* (2002) evidenced that the damage was independent on the source energy in a 9-17 keV range, suggesting that the risk of membrane damage is intrinsic to the technique and cannot be reduced by modifying X-ray energy level without losing image quality and resolution.

In addition to disruption of cell membranes, our data indicate that microCT scans negatively affect RNA quality. This is also not unexpected, as ionizing radiation is known to induce significant alterations on nucleic acids, often resulting in DNA double strand breaks (Rothkamm & Löbrich, 2003; Han & Yu, 2009) and ROS-mediated DNA/RNA disruption (van Huystee *et al.*, 1968; Tominaga *et al.*, 2004), finally leading to severe RNA and/or protein damage (Daly, 2012). Our data from plants are in line with findings obtained on animal cell models, and suggest that, as a consequence of RNA damage, protein synthesis can be impaired in stem parenchyma cells after microCT scans.

Both membrane damage and RNA degradation were observed in three studied species, but the susceptibility to X-rays damage was species-specific. *C. arabica* was damaged by a single scan, while two-three scans were necessary to produce significant effects in other two species. It is possible that not all microCT experiments performed on different species and reported in the literature are affected to the same extent by harmful radiation effects, potentially explaining the observed range of hydraulic recovery in different species (Choat *et al.*, 2015; Knipfer *et al.*, 2015; Charrier *et al.*, 2016; Brodersen *et al.*, 2018). Our findings call for a careful reassessment of previous conclusions, based on dedicated experiments to evaluate the susceptibility of individual species to the specific experimental conditions adopted.

Our data show that multiple microCT scans lead to disruption of fundamental cellular functions and processes. Hence, microCT investigation of phenomena that depend on physiological activity of living cells may produce erroneous results and lead to incorrect conclusions. This probably

applies to conduit refilling, which has been suggested to occur via secretion of sugars into embolized conduits by phloem and vessel-associated parenchyma cells to generate the osmotic forces necessary to counterbalance eventual residual tension in still functioning elements (Secchi & Zwieniecki, 2012). Such a mechanism requires the activation of genes encoding key proteins involved in carbohydrate metabolism pathways and membrane transport of inorganic ions, sugar molecules, and water (Secchi *et al.*, 2011; Perrone *et al.*, 2012; Chitarra *et al.*, 2014; Secchi *et al.*, 2016). Thus, failure in detecting embolism reversal in microCT experiments, when involving repeated scans of the same plant subjected to drought stress and then re-irrigated (Choat *et al.*, 2015; Knipfer *et al.*, 2015; Charrier *et al.*, 2016; Knipfer *et al.*, 2017), might arise from X-ray induced damage to living cells. We strongly suggest that such evidence should be re-evaluated in the light of our findings, and also recommend that xylem vulnerability or recovery curves generated by microCT should be based on sets of different plants, so that a single plant at any given water status or physiological stage is scanned and observed only once if the species is susceptible to applied radiation levels. Although this approach might raise doubts on the advantages of microCT as an alternative or complementary technique with respect to classical hydraulic measurements, it would still yield important information or confirmation on the functional status of conduits with no risk of bias due to cutting procedures.

MicroCT observations are increasingly used to observe xylem embolism build-up during plant dehydration. It is assumed that embolism spreads by aspiration of air through the pores of inter-conduit remnants of primary cell walls and middle lamella (pit membranes). Thus, the validity of observations of embolism spread is seemingly not challenged by our findings, unless X-rays disrupt and alter the structure and porosity of pit membranes, leading to erroneous estimates of embolism vulnerability. Also, damage to living cells might result in wound responses leading to rapid filling of xylem conduits with gels (Crews *et al.*, 2003; Soukup & Votrubová, 2005; Marañón-Jiménez *et al.*, 2017; Che-Husin *et al.*, 2018; Jacobsen *et al.*, 2018). Such an effect would cause conduits to appear filled with a liquid phase even though non-conducting (Pratt & Jacobsen, 2018), leading to overestimate plant resistance to xylem embolism. The occurrence and relevance of these effects should be evaluated by future studies.

ACKNOWLEDGEMENTS

This study was made possible by Elettra-Sincrotrone Trieste, which allowed and funded access to the SYRMEP beamline (proposals nr. 20165201 and nr. 20165277). We thank Birgit Dämon (University of Innsbruck) for assistance during experiments at SYRMEP, Cinzia Bertea and Cristina Morabito (University of Torino) for help with Bionalyzer assay.

AUTHOR CONTRIBUTIONS

A.N., F.S., M.Z., and S.M. planned and designed the research. All Authors contributed to perform experiments and analyze data. F.P., A.N. and F.S. wrote the manuscript, with contribution and revision by all Authors.

REFERENCES

Anderegg WRL, Berry JA, Smith DD, Sperry JS, Anderegg LDL, Field CB. 2011. The roles of hydraulic and carbon stress in a widespread climate-induced forest die-off. *Proceedings of the National Academy of Sciences USA* **109:** 233-237.

Beikircher B, Mayr S. 2016. Avoidance of harvesting and sampling artefacts in hydraulic analyses: a protocol tested on *Malus domestica*. *Tree Physiology* **36:** 797-803.

Brodersen CR, Knipfer T, McElrone AJ. 2018. In vivo visualization of the final stages of xylem vessel refilling in grapevine (*Vitis vinifera*) stems. *New Phytologist* **217:** 117-126.

Brodersen CR, McElrone AJ. 2013. Maintenance of xylem network transport capacity: a review of embolism repair in vascular plants. *Frontiers in Plant Science* **4:** 108.

Brodersen CR, McElrone AJ, Choat B, Matthews MA, Shackel KA. 2010. The dynamics of embolism repair in xylem: in vivo visualizations using high-resolution computed tomography. *Plant Physiology* **154:** 1088-1095.

Brodribb TJ, Skelton RP, McAdam SAM, Bienaimé D, Lucani CJ, Marmottant P. 2016. Visual quantification of embolism reveals leaf vulnerability to hydraulic failure. *New Phytologist* **209:** 1403-1409.

Cao G, Zhang M, Miao J, Li W, Wang J, Lu D, Xia J. 2015. Effects of X-ray and carbon ion beam irradiation on membrane permeability and integrity in *Saccharomyces cerevisiae* cells. *Journal of Radiation Research* **56:** 294-304.

Chang S, Puryear J, Cairney J. 1993. A simple and efficient method for isolating RNA from pine tree. *Plant Molecular Biology Report* **11:** 113-116.

Charrier G, Torres-Ruiz JM, Badel E, Burlett R, Choat B, Cochard H, Delmas CEL, Domec JC, Jansen S, King A, Lenoir N, Martin-StPaul N, Gambetta GA, Delzon S. 2016. Evidence for hydraulic vulnerability segmentation and lack of xylem refilling under tension. *Plant Physiology* **172:** 1657-1668.

Che-Husin NM, Joyce DC, Irving DE. 2018. Gel xylem occlusions decrease hydraulic conductance of cut *Acacia holosericea* foliage stems. *Postharvest Biology and Technology* **135:** 27-37.

Cheng A, Caffrey M. 1996. Free radical mediated X-ray damage of model membranes. *Biophysical Journal* **70:** 2212-2222.

Cherezov V, Riedl KM, Caffrey M. 2002. Too hot to handle? Synchrotron X-ray damage of lipid membranes and mesophases. *Journal of Synchrotron Radiation* **9:** 333-341.

Chitarra W, Balestrini R, Vitali M, Pagliarani C, Perrone I, Schubert A, Lovisolo C. 2014. Gene expression in vessel−associated cells upon xylem embolism repair in *Vitis vinifera* L. petioles. *Planta* **239:** 887-899.

Choat B, Brodersen CR, McElrone AJ. 2015. Synchrotron X-ray microtomography of xylem embolism in *Sequoia sempervirens* saplings during cycles of drought and recovery. *New Phytologist* **205:** 1095-1105.

Choat B, Badel E, Burlett R, Delzon S, Cochard H, Jansen S. 2016. Noninvasive measurement of vulnerability to drought-induced embolism by X-ray microtomography. *Plant Physiology* **170:** 273-282.

Cochard H, Badel E, Herbette S, Delzon S, Choat B, Jansen S. 2013. Methods for measuring plant vulnerability to cavitation: a critical review. *Journal of Experimental Botany* **64:** 4779-4791.

Cochard H, Delzon S, Badel E. 2015. X-ray microtomography (microCT): a reference technology for high-resolution quantification of xylem embolism in trees. *Plant, Cell & Environment* **38:** 201-206.

Crews LJ, McCully ME, Canny MJ. 2003. Mucilage production by wounded xylem tissue of maize roots - time course and stimulus. *Functional Plant Biology* **30:** 755-766.
Daly MJ. 2012. Death by protein damage in irradiated cells. *DNA Repair* **11:** 12-21.
Dhondt S, Vanhaeren H, Van Loo D, Cnudde V, Inzé D. 2010. Plant structure visualization by high-resolution X-ray computed tomography. *Trends in Plant Science* **15:** 419-422.
Ewers FW, Fisher JB. 1989. Techniques for measuring vessel lengths and diameters in stems of woody plants. *American Journal of Botany* **76:** 645-656.
Fukuda K, Kawaguchi D, Aihara T, Ogasa MY, Miki NH, Haishi T, Umebayashi T. 2015. Vulnerability to cavitation differs between current-year and older xylem: non-destructive observation with a compact magnetic resonance imaging system of two deciduous diffuse-porous species. *Plant, Cell & Environment* **38:** 2508-2518.
Hacke UG, Venturas MD, MacKinnon ED, Jacobsen AL, Sperry JS, Pratt RB. 2015. The standard centrifuge method accurately measures vulnerability curves of long-vesselled olive stems. *New Phytologist* **205:** 116-127.
Han W, Yu KN. 2009. Response of cells to ionizing radiation. In: Tjong SC, ed. *Advances in Biomedical Sciences and Engineering*. Bentham Science Publisher Ltd, 204-262.
Hember RA, Kurz WA, Coops NC. 2017. Relationships between individual-tree mortality and water-balance variables indicate positive trends in water stress-induced tree mortality across North America. *Global Change Biology* **23:** 1691-1710.
Hochberg U, Herrera JC, Cochard H, Badel E. 2016. Short-time xylem relaxation results in reliable quantification of embolism in grapevine petioles and sheds new light on their hydraulic strategy. *Tree Physiology* **36:** 748-755.
Jacobsen AL, Pratt RB. 2012. No evidence for an open vessel effect in centrifuge-based vulnerability curves of a long-vesselled liana (*Vitis vinifera*). *New Phytologist* **194:** 982-990.
Jacobsen AL, Valdovinos-Ayala J, Pratt RB. 2018. Functional lifespans of xylem vessels: Development, hydraulic function, and post-function of vessels in several species of woody plants. *American Journal of Botany* **105:** 142-150.
Jansen S, Schuldt B, Choat B. 2015. Current controversies and challenges in applying plant hydraulic techniques. *New Phytologist* **205:** 961-964.
Jensen KH, Berg-Sørensen K, Bruus H, Holbrook NM, Liesche J, Schulz A, Zwieniecki MA, Bohr T. 2016. Sap flow and sugar transport in plants. *Reviews of Modern Physics* **88:** 035007.
Klein T, Zeppel MJB, Anderegg WRL, Bloemen J, De Kauwe MG, Hudson P, Ruehr NK, Powell TL, von Arx G, Nardini A. 2018. Xylem embolism refilling and resilience against drought-induced mortality in woody plants: processes and trade-offs. *Ecological Research* doi:10.1007/s11284-018-1588-y
Knipfer T, Brodersen CR, Zedan A, Kluepfel DA, McElrone AJ. 2015. Patterns of drought-induced embolism formation and spread in living walnut saplings visualized using X-ray microtomography. *Tree Physiology* **35:** 744-755.
Knipfer T, Cuneo IF, Earles JM, Reyes C, Brodersen CR, McElrone AJ. 2017. Storage compartments for capillary water rarely refill in an intact woody plant. *Plant Physiology* **175:** 1649-1660.
Köteles GJ. 1982. Radiation effects on cell membranes. *Radiation and Environmental Biophysics* **21:** 1-18.
Losso A, Beikircher B, Dämon B, Kikuta S, Schmid P, Mayr S. 2017. Xylem sap surface tension may be crucial for hydraulic safety. *Plant Physiology* **175:** 1135-1143.
Maherali H, Pockman WT, Jackson RB. 2004. Adaptive variation in the vulnerability of woody plants to xylem cavitation. *Ecology* **85:** 2184-2199.
Marañón-Jiménez S, Van den Bulcke J, Piayda A, Van Acker J, Cuntz M, Rebmann C, Steppe K. 2017. X-ray computed microtomography characterizes the wound effect that causes sap flow underestimation by thermal dissipation sensors. *Tree Physiology* **38:** 288-302.
Mayr S, Schmid P, Laur J, Rosner S, Charra-Vaskou K, Dämon B, Hacke UG. 2014. Uptake of water via branches helps timberline conifers refill embolized xylem in late winter. *Plant Physiology* **164:** 1731-1740.

Nardini A, Salleo S, Jansen S. 2011. More than just a vulnerable pipeline: xylem physiology in the light of ion-mediated regulation of plant water transport. *Journal of Experimental Botany* **62:** 4701-4718.

Nardini A, Savi T, Losso A, Petit G, Pacilè S, Tromba G, Mayr S, Trifilò P, Lo Gullo MA, Salleo S. 2017. X-ray microtomography observations of xylem embolism in stems of *Laurus nobilis* are consistent with hydraulic measurements of percentage loss of conductance. *New Phytologist* **213:** 1068-1075.

Nardini A, Savi T, Trifilò P, Lo Gullo MA. 2018. Drought stress and the recovery from xylem embolism in woody plants. *Progress in Botany* **79:** 197-231.

Nguyen PK, Lee WH, Li YF, Hong WX, Hu S, Chan C, Liang G, Nguyen I, Ong SG, Churko J, Wang J, Altman RB, Fleischmann D, Wu JC. 2015. Assessment of the radiation effects of cardiac CT angiography using protein and genetic biomarkers. *JACC: Cardiovascular Imaging* **8:** 873-884.

Nolf M, Lopez R, Peters JMR, Flavel RJ, Koloadin LS, Young IM, Choat B. 2017. Visualization of xylem embolism by X-ray microtomography: a direct test against hydraulic measurements. *New Phytologist* **214:** 890-898.

Ogasa MY, Utsumi Y, Miki NH, Yazaki K, Fukuda K. 2016. Cutting stems before relaxing xylem tension induces artefacts in *Vitis coignetiae*, as evidenced by magnetic resonance imaging. *Plant, Cell & Environment* **39:** 329-337.

Pajor R, Fleming A, Osborne CP, Rolfe SA, Sturrock CJ, Mooney SJ. 2013. Seeing space: visualization and quantification of plant leaf structure using X-ray micro-computed tomography. *Journal of Experimental Botany* **64:** 385-390.

Perrone I, Pagliarani C, Lovisolo C, Chitarra W, Roman F, Schubert A. 2012. Recovery from water stress affects grape leaf petiole transcriptome. *Planta* **235:** 1383-1396.

Pratt RB, Jacobsen AL. 2018. Identifying which conduits are moving water in woody plants: a new HRCT-based method. *Tree Physiology* doi:10.1093/treephys/tpy034

Rothkamm K, Löbrich M. 2003. Evidence for a lack of DNA double-strand break repair in human cells exposed to very low X-ray doses. *Proceedings of the National Academy of Sciences USA* **100:** 5057-5062.

Savi T, Dal Borgo A, Love VL, Andri S, Tretiach M, Nardini A. 2016. Drought versus heat: what's the major constraint on Mediterranean green roof plants? *Science of the Total Environment* **566:** 753-760.

Savi T, Miotto A, Petruzzellis F, Losso A, Pacilè S, Tromba G, Mayr S, Nardini A. 2017. Drought-induced embolism in stems of sunflower: a comparison of in vivo micro-CT observations and destructive hydraulic measurements. *Plant Physiology & Biochemistry* **120:** 24-29.

Schroeder A, Mueller O, Stocker S, Salowsky R, Leiber M, Gassmann M, Lightfoot S, Menzel W, Granzow M, Ragg T. 2006. The RIN: an RNA integrity number for assigning integrity values to RNA measurements. *BMC Molecular Biology* **7:** 3.

Scoffoni C, Sack L. 2015. Are leaves 'freewheelin'? Testing for a Wheeler-type effect in leaf xylem hydraulic decline. *Plant, Cell & Environment* **38:** 534-543.

Secchi F, Gilbert ME, Zwieniecki MA. 2011. Transcriptome response to embolism formation in stems of *Populus trichocarpa* provides insight into signaling and the biology of refilling. *Plant Physiology* **157:** 1419-1429.

Secchi F, Pagliarani C, Zwieniecki MA. 2017. The functional role of xylem parenchyma cells and aquaporins during recovery from severe water stress. *Plant, Cell & Environment* **40:** 858-871.

Secchi F, Zwieniecki MA. 2012. Analysis of xylem sap from functional (nonembolized) and nonfunctional (embolized) vessels of *Populus nigra*: chemistry of refilling. *Plant Physiology* **160:** 955-964.

Secchi F, Zwieniecki MA. 2016. Accumulation of sugars in the xylem apoplast observed under water stress conditions is controlled by xylem pH. *Plant Cell & Environment* **39:** 2350-2360.

Shen F, Cheng Y, Zhang L, Gao R, Shao X. 2015. Experimental study of the types of cavitation by air seeding using light microscopy. *Tree Physiology* **35:** 1325-1332.

Soukup AS, Votrubová O. 2005. Wound-induced vascular occlusions in tissues of the reed *Phragmites australis*: their development and chemical nature. *New Phytologist* **167:** 415-424.

Sperry JS, Donnelly JR, Tyree MT. 1988. A method for measuring hydraulic conductivity and embolism in xylem. *Plant, Cell & Environment* **11:** 35-40.

Tominaga H, Kodama S, Matsuda N, Suzuki K, Watanabe M. 2004. Involvement of reactive oxygen species (ROS) in the induction of genetic instability by radiation. *Journal of Radiation Research* **45:** 181-188.

Trifilò P, Raimondo F, Lo Gullo MA, Barbera PM, Salleo S, Nardini A. 2014. Relax and refill: xylem rehydration prior to hydraulic measurements favours embolism repair in stems and generate artificially low PLC values. *Plant, Cell & Environment* **37:** 2491-2499.

Tyree MT, Salleo S, Nardini A, Lo Gullo MA, Mosca R. 1999. Refilling of embolized vessels in young stems of Laurel. Do we need a new paradigm? *Plant Physiology* **120:** 11-21.

Van Huystee RB, Jachymczyk W, Tester CF, Cherry JH. 1968. X-irradiation effects on protein synthesis and synthesis of messenger ribonucleic acid from peanut cotyledons. *The Journal of Biological Chemistry* **243:** 2315-2320.

Venturas MD, MacKinnon ED, Jacobsen AL, Pratt RB. 2015. Excising stem samples underwater at native tension does not induce xylem cavitation. *Plant, Cell & Environment* **38:** 1060-1068.

Venturas MD, Sperry JS, Hacke UG. 2017. Plant xylem hydraulics: what we understand, current research, and future challenges. *Journal of Integrative Plant Biology* **59:** 356-389.

Wheeler JK, Huggett BA, Tofte AN, Rockwell FE, Holbrook NM. 2013. Cutting xylem under tension or supersaturated with gas can generate PLC and the appearance of rapid recovery from embolism. *Plant, Cell & Environment* **36:** 1938-1949.

Zimmermann MH. 1983. Xylem structure and the ascent of sap. Springer Verlag, Berlin.

Zwieniecki MA, Melcher PJ, Ahrens ET. 2013. Analysis of spatial and temporal dynamics of xylem refilling in *Acer rubrum* L. using magnetic resonance imaging. *Frontiers in Plant Science* **4:** 265.

Zwieniecki MA, Melcher PJ, Holbrook NM. 2001. Hydrogel control of xylem hydraulic resistance in plants. *Science* **291:** 1059-1062.

Zwieniecki MA, Secchi F. 2015. Threats to xylem hydraulic function of trees under 'new climate normal' conditions. *Plant, Cell & Environment* **38:** 1713-1724.

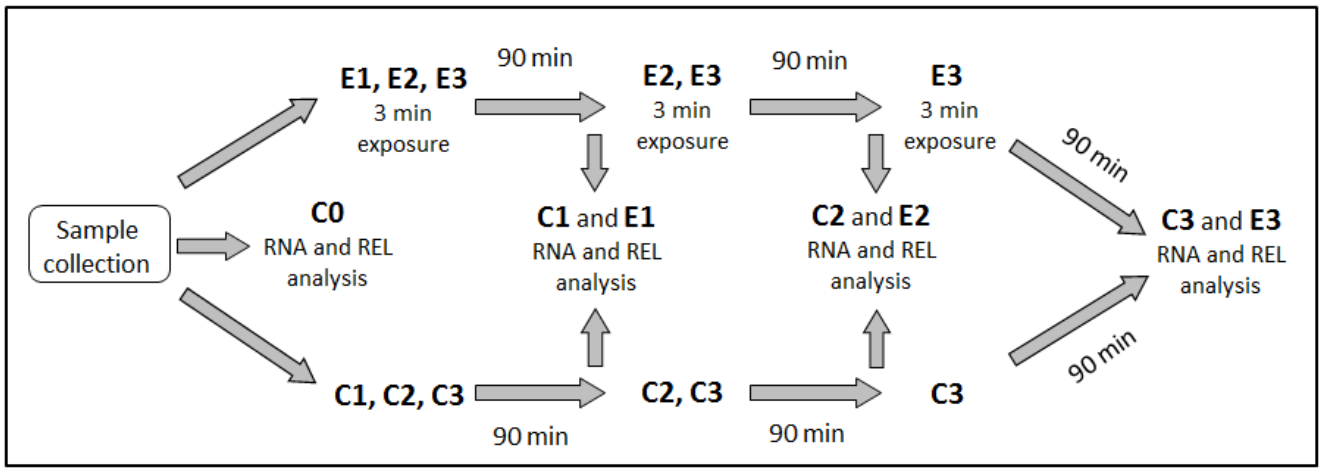

Fig. 1: Experiment time line. C0: control samples i) immediately used for REL measurements or ii) frozen in liquid nitrogen and kept at -80 °C until RNA analysis. C1: samples excised from stems and stored at laboratory temperature until segments from group E1 were ready, then processed for REL or RNA analyses (see above). Samples C1, C2 and C3 were prepared to check eventual time-related trends in cellular damage not associated to X-rays exposure. E1: samples exposed to a single 3 min microCT scan (see below), maintained for 90 min at laboratory temperature to allow eventual damage build-up, then processed for REL or RNA analyses. C2: samples excised from stems and stored at laboratory temperature until samples from group E2 were ready, then processed for REL or RNA measurements. E2: samples exposed to two successive microCT scans (90 min between each exposure and after the last one), then processed for REL or RNA measurements. C3: samples excised from stems and stored at laboratory temperature until samples from group E3 were ready, then processed for REL or RNA measurements. E3: samples exposed to three successive microCT scans (90 min between each exposure and after the last one), then processed for REL or RNA measurements.

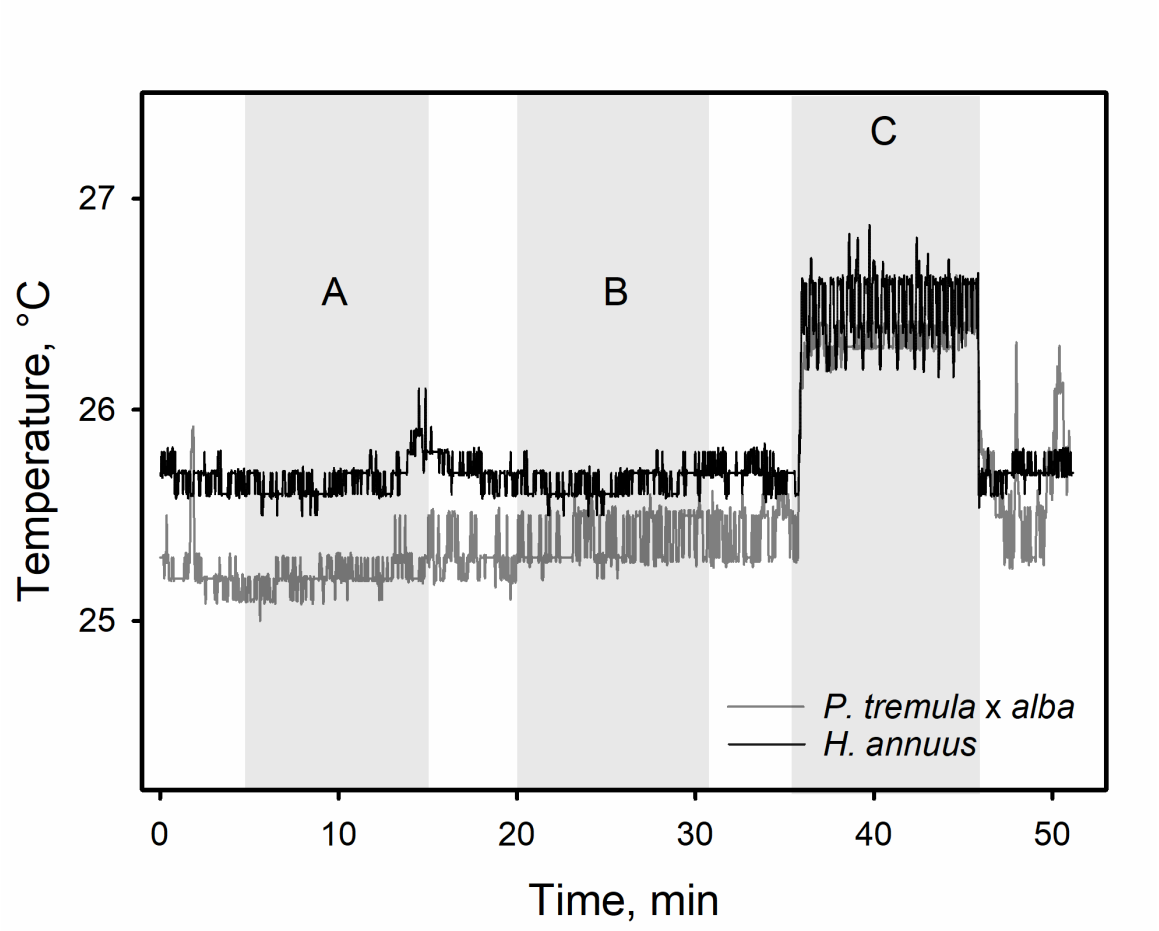

Fig. 2: Temperature changes over time in irradiated stems of *P. tremula* x *alba* (grey line) and *H. annuus* (black line) at 8 mm (A), 3 mm (B) and at the same position (C) of irradiation point.

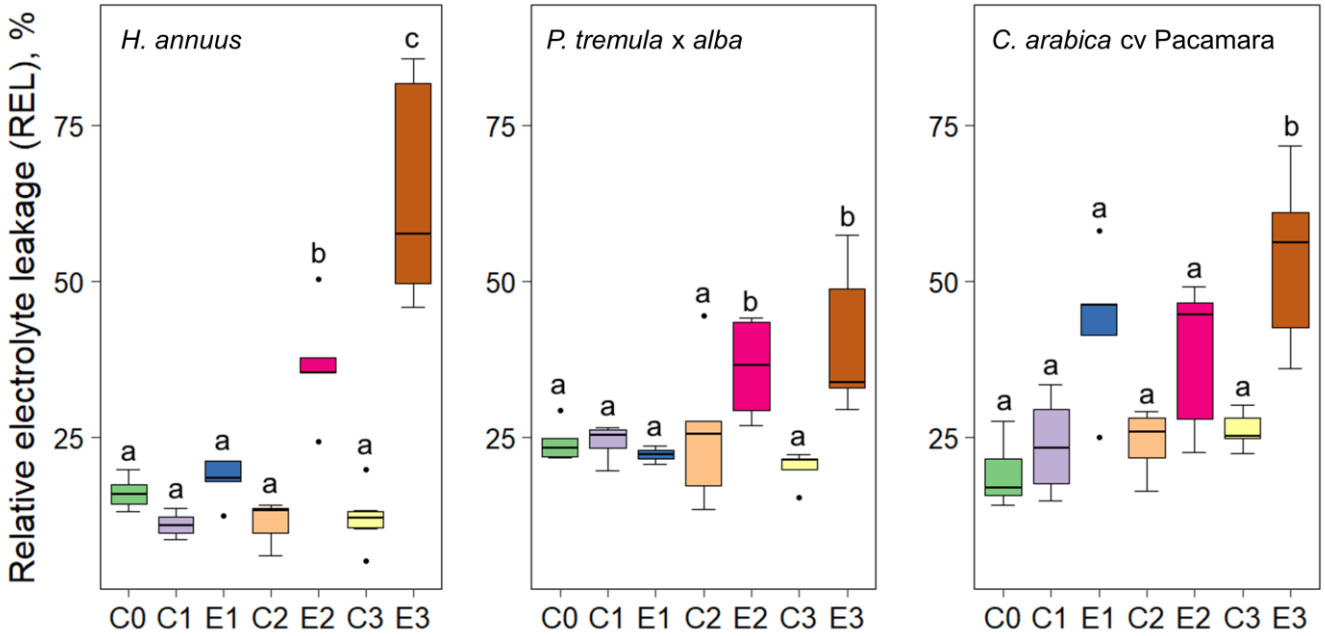

Fig. 3: Median values, 25th and 75th percentiles of relative electrolyte leakage (REL) in control and exposed sample groups in *H. annuus*, *P. tremula x alba* and in *C. arabica* cv. Pacamara. Different letters indicate statistical significant differences among groups ($p<0.05$).

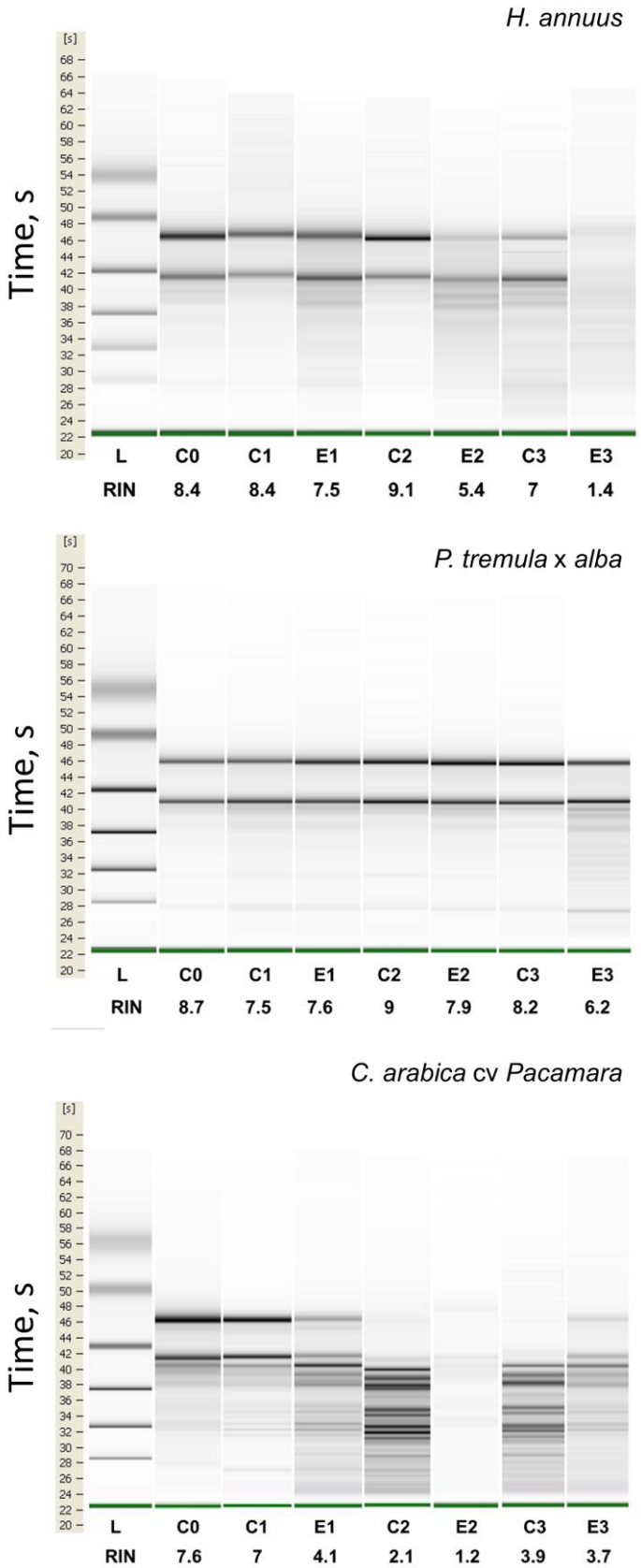

Fig. 4: Evaluation of RNA integrity by Bioanalyzer assay. For each RNA sample, extracted from control (C) or exposed plant stems (E), the related RIN (RNA integrity number) is provided below each lane of the gel. L = ladder.